applied sciences

MDPI

Article

Real-Time Vehicle Energy Management System Based on Optimized Distribution of Electrical Load Power

Yuefei Wang [1,2,*], Hao Hu [1], Li Zhang [1], Nan Zhang [1] and Xuhui Sun [1]

[1] School of Mechanical and Automotive Engineering, Hefei University of Technology, Hefei 230009, China; huhaohowe@hotmail.com (H.H.); 77zhangli@hfut.edu.cn (L.Z.); znhfut@hotmail.com (N.Z.); sunxuhuiroro@yahoo.com (X.S.)

[2] Engineering Research Center of Safety Critical Industrial Measurement and Control Technology of Ministry of Education, Hefei University of Technology, Hefei 230009, China

* Correspondence: yuefeiw@hfut.edu.cn; Tel.: +86-551-6290-1397

Academic Editor: Minho Shin
Received: 25 July 2016; Accepted: 26 September 2016; Published: 2 October 2016

Abstract: As a result of severe environmental pressure and stringent government regulations, refined energy management for vehicles has become inevitable. To improve vehicle fuel economy, this paper presents a bus-based energy management system for the electrical system of internal combustion engine vehicles. Both the model of an intelligent alternator and the model of a lead-acid battery are discussed. According to these models, the energy management for a vehicular electrical system is formulated as a global optimal control problem which aims to minimize fuel consumption. Pontryagin's minimum principle is applied to solve the optimal control problem to realize a real-time control strategy for electrical energy management in vehicles. The control strategy can change the output of the intelligent alternator and the battery with the changes of electrical load and driving conditions in real-time. Experimental results demonstrate that, compared to the traditional open-loop control strategy, the proposed control strategy for vehicle energy management can effectively reduce fuel consumption and the fuel consumption per 100 km is decreased by approximately 1.7%.

Keywords: energy management; power distribution; real-time control strategy; fuel economy

1. Introduction

To address energy scarcity and environmental pollution, many countries have issued and implemented strict standards of vehicle energy consumption and automotive exhaust emissions. Although new energy vehicles (NEV) can effectively meet these standards, replacing the internal combustion engine (ICE) vehicle with NEV is difficult because of technical issues, such as small battery capacity, long charging time, and high battery cost. The automotive industry is striving to improve the efficiency of the energy management technology for ICE vehicles to ensure better fuel economy and less harmful exhaust emissions [1].

Today, the online energy management method has become an important research direction to improve vehicle fuel economy. An energy management strategy for plug-in hybrid electric vehicles (PHEV) was proposed by Zheng [2], which used Pontryagin's minimum principle (PMP) to split power. Hanane [3] predicted the future power demand of vehicle through a Markov chain model and then calculated power distribution between the supercapacitor and fuel cell through PMP. Similarly, Hou [4] presented an optimal energy management strategy based on an approximate PMP algorithm for PHEVs. An adaptive supervisory controller was proposed by Simona [5] based on PMP for the online energy management optimization of PHEV. For the implementation of an energy management strategy, Zou [6] concluded that PMP computation time is significantly less than that of dynamic programming under the same conditions.

Although the aforementioned methods can improve fuel economy effectively, they cannot directly extend to ICE vehicles because of distinctively different structures of vehicle electrical systems. The power system of ICE vehicles is composed of an alternator and a battery. An intelligent control strategy of a vehicular alternator was observed in the studies by Kong [7]. The strategy reduced fuel consumption by adjusting the working mode of the alternator. Yang [8] investigated the methods of battery management that partitions the working states of the battery and monitor. However, previous studies concentrated less on the collaborative work between the alternator and the battery. Colin [9] and Jeremy [10] presented a model-based supervisory energy management strategy, respectively. The strategy attempted to control the duty cycle of the alternator to meet the instantaneous demand of load current. However, the strategy seems to be difficult to implement in engineering. For ICE vehicles, a vehicular energy management system based on local interconnection network (LIN) bus was proposed by Wang [11], in which a double fuzzy controller was designed to recover braking energy. However, the controller only controlled the output of the alternator according to the vehicle speed and the state of the battery charge, and it never considered the variation of the electrical load.

Based on previous studies, a bus-based real-time energy management system is proposed for the ICE vehicle electrical system, and its real-time energy management strategy based on PMP is presented. The proposed strategy optimally distributes the power demand of electrical load between the intelligent alternator and the battery so that better fuel economy can be obtained.

The remainder of this paper is organized as follows: Section 2 describes the bus-based power management system, and the vehicular electrical system is modeled through experiments in Section 3; the real-time energy management strategy for the power management system is proposed in Section 4, and Section 5 discusses the experimental results; finally, conclusions are provided in Section 6.

2. Bus-Based Energy Management System

2.1. Structure of the System

An energy management system is considered, as shown in Figure 1. This system consists of an energy management controller (Jianghuai Auto., Hefei, China), an intelligent battery sensor (IBS, Hella, Lippstadt, Germany), and an intelligent alternator (Bosch, Stuttgart, Germany), which communicate with each other through the LIN bus. The body controller module (BCM), engine management system (EMS), and other control units, such as the controller for the air conditioning, are located in the controller area network (CAN). Various control signals between the LIN and CAN buses are transferred by the gateway BCM.

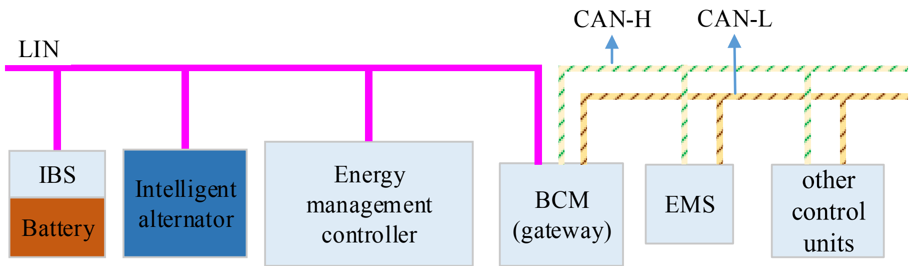

Figure 1. Structure of energy management system.

The intelligent alternator is the main power source, and the battery is the auxiliary power source, in vehicles. The IBS collects the voltage and current, and calculates the state of charge (SoC) of the battery in real-time. The BCM sends the on-off state of electrical loads, while the EMS provides the vehicle and engine speed, and engine torque. When the energy management controller receives the aforementioned information, it will optimize the distribution of the alternator output power and battery output power to maintain the best fuel consumption.

2.2. The Battery SoC and Intelligent Alternator Operation Mode

The battery charge level is divided into three modes: deficient, working, and recovery [8]. When the battery SoC is in the deficient mode, the battery should be charged quickly. When the battery SoC is in the working or recovery modes, the charging and discharging of the battery should be controlled according to driving situations and the total power demand of the electrical loads. The recovery mode is considered to provide sufficient capacity for braking energy recovery. All battery modes are shown in Figure 2.

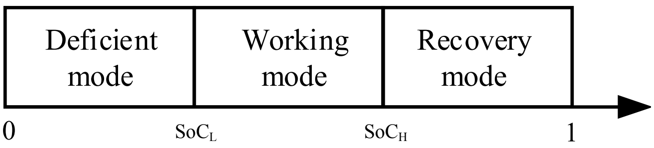

Figure 2. Modes of battery SoC.

The intelligent alternator has four operation modes, as shown in Figure 3. These modes are ready, pre-excitation, voltage regulation, and excitation off. The ready mode is activated only when the sleep command is received from the energy management controller, and the rotational speed of the alternator n_G does not exceed the rotational speed threshold n_0. The alternator switches into pre-excitation mode if a valid set voltage U_S is more than the voltage threshold U_0 and $n_G < n_0$. For the pre-excitation mode, if n_G exceeds n_0, the voltage regulation state is entered, and the output voltage of alternator can be regulated. Without an activation command, and if the rotational speed of the alternator n_G exceeds the rotational speed n_1 ($n_1 > n_0$), the alternator switches into the voltage regulation state directly. When the command of excitation off from the energy management controller is received, the alternator stops the excitation until a valid new set voltage U_S is received.

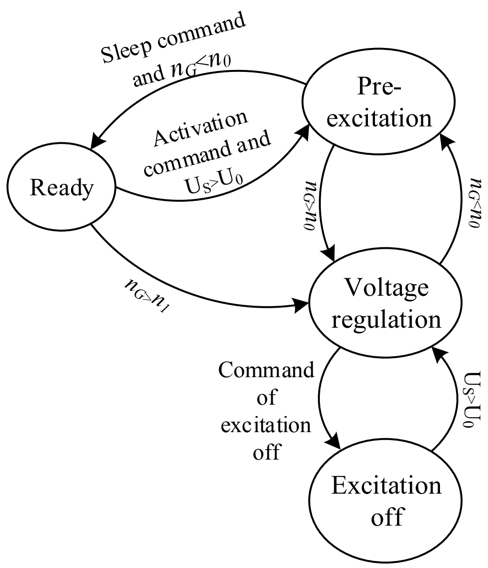

Figure 3. Intelligent alternator operation mode.

When more electrical loads are switched on, and the SoC of battery is in the recovery mode, the energy management controller reduces the alternator voltage or closes its excitation and makes the battery work for the electrical loads to maintain a low level of engine fuel consumption. When the battery SoC is in the working or recovery modes, the higher voltage of the alternator is regulated by the energy management controller to recover the braking energy. When the battery SoC is in the deficient mode, the energy management controller raises the charging voltage of the battery, so the battery SoC can return to the working mode quickly.

3. Modeling of Vehicle Power System

3.1. Intelligent Alternator Model

The intelligent alternator model mainly consists of three interrelated variables: output voltage (V_G), output power (P_G), and rotational speed of the engine (n). Their relation can be expressed as follows:

$$P_G = P_G(n, V_G). \tag{1}$$

The model of an intelligent alternator can be obtained by an experiment. Figure 4 shows the relation between the output power of the intelligent alternator, the rotational speed of the engine, and the output voltage of the intelligent alternator [9,10]. Figure 5 presents the mapping characteristic curve of the engine, which shows the correlation between the rotational speed n of the engine, torque T of the engine, and fuel consumption rate.

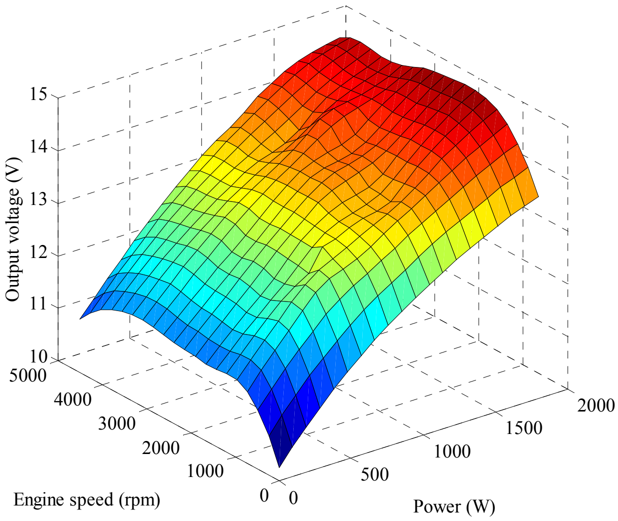

Figure 4. Intelligent alternator model.

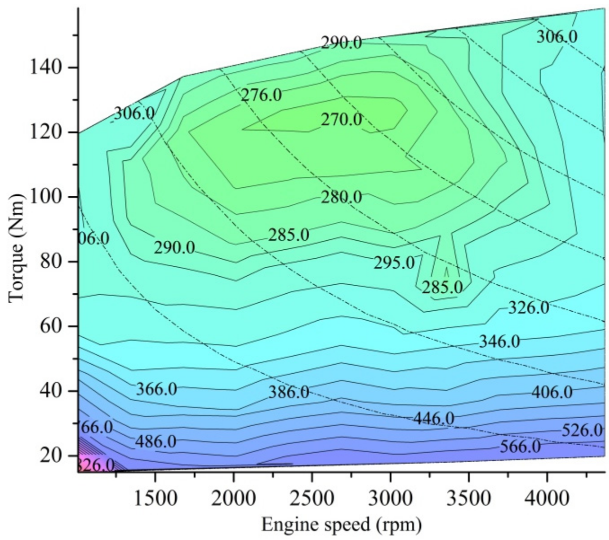

Figure 5. Mapping characteristic curve of the engine.

3.2. Battery Model

The battery is an essential component of the vehicle power system. In this paper, a 12 V lead-acid battery is considered. The equivalent circuit model of the battery, as shown in Figure 6, is used widely in battery analysis [12]. In this circuit model, where V_B is the output voltage of the battery, V_o is the open circuit voltage (OCV) of the battery (i.e., electromotive force), R_i is the internal resistance of the battery, and I_B is the battery current. The relation among V_o, R_i, and I_B can be expressed as Equation (2).

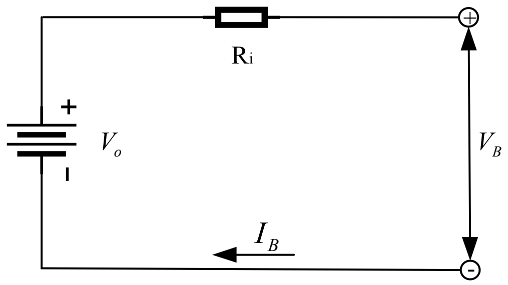

Figure 6. Equivalent circuit of a battery.

The battery SoC is an important parameter for the energy management system [13]. It can be calculated through Equation (3):

$$V_B(t) = V_o(t) - R_i I_B(t), \tag{2}$$

$$SoC\,(t) = SoC_0 - \frac{\beta}{Ah_{nom}} \int_{t_0}^{t} I_B(t)dt, \tag{3}$$

where SoC_0 is the value of SoC at t_0, Ah_{nom} is the nominal capacity of the battery, and β is the charge-discharge efficiency factor of the battery. When the battery is charging, $\beta \leq 1$; when the battery is discharging, $\beta \geq 1$. Through charging and discharging experiments, β can be obtained. Furthermore, the correlation curve of SoC-OCV, as established by experiments [14], is used to obtain SoC_0 or the corresponding V_o. Figure 7 shows the SoC-OCV curve at temperature 25 °C, −30 °C, and 70 °C. Generally, the SoC-OCV curve at 25 °C is adopted in practical applications.

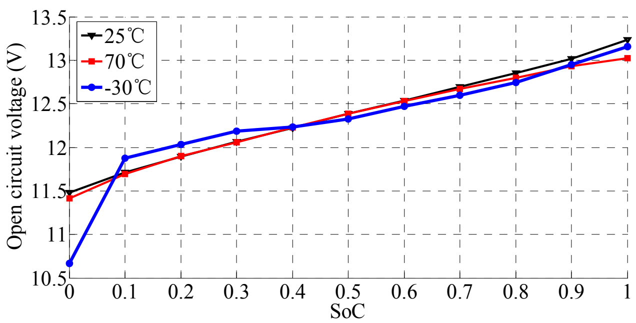

Figure 7. SoC-OCV correlation curve.

4. Real-Time Energy Management Strategy

4.1. Problem Description

The energy management of the vehicle electrical system is a type of optimization problem with boundary conditions in a specific driving cycle. For the optimal fuel economy, the energy management strategy of the vehicle electrical system aims to control the output power of the battery and the alternator, and to maintain the battery SoC within the working mode.

Therefore, the energy management strategy can be simplified as the control of single degree of freedom. The system controlled variable $u(t)$ is the battery power $P_B(t)$, the system state variable $x(t)$ is the battery SoC, and the control objective is to minimize fuel consumption of the engine. Accordingly, the objective function of the energy management strategy under a driving cycle in the duration $[t_0, t_f]$ is expressed as follows [15]:

$$J = \min\left(\int_{t_0}^{t_f} \dot{m}_f\left(x(t), u(t), t\right) dt\right), \tag{4}$$

where $\dot{m}_f$ is the fuel consumption rate of the engine, and its value can be obtained from the characteristic curve of engine mapping in Figure 5 based on the rotational speed n of the engine and torque T.

To simplify the study, if we neglect the time-variant parameters of the battery, such as ohmic resistance and polarization resistance, the system state equation can be derived according to Equations (2) and (3), as follows:

$$\dot{x}\left(t\right) = f\left(x\left(t\right), u\left(t\right), t\right) = -\frac{I_B(x(t), u(t))\beta}{3600Ah_{nom}}, \tag{5}$$

$$I_B(t) = \frac{V_o\left(x\right) - \sqrt{V_o^2\left(x\right) - 4R_iP_B(t)}}{2R_i}, \tag{6}$$

where $P_B(t)$ expresses the charging and discharging power of the battery at t moment, and $V_o(x)$ is OCV when SoC is x.

To avoid overcharging and overdischarging of the battery, the final and initial values of SoC are generally required to be equal, and the battery constantly works within a certain range. In addition, the output power should meet certain constrained conditions when controlled by the working capacity of the alternator and battery:

$$\begin{cases} x\left(t_0\right) = x_0 \\ x\left(t_f\right) = x_f = x_0 \\ x\left(t\right) \in \left[x_{min}, x_{max}\right] \\ P_L\left(t\right) = P_B\left(t\right) + P_G\left(t\right) \\ P_G\left(t\right) \in \left[0, P_{max}\right] \\ P_B \in \left[P_{B\_min}, P_{B\_max}\right] \end{cases}, \tag{7}$$

where $x_{\min}$ and $x_{\max}$ are, respectively, the upper and lower limits of the battery SoC. P_L is the power of thre electrical load; $P_{\max}$ is the maximum output power of the alternator; and $P_{B\_\min}$ and $P_{B\_\max}$ are the maximum charging power and maximum discharging power of the battery, respectively.

4.2. PMP-Based Solution

According to the aforementioned objective function, PMP can convert the global optimum problem into a local one by a series of constrained conditions. The following Hamiltonian function [15] expresses the objective function in Equation (8):

$$H\left(x, u, \gamma, \varphi, t\right) = \dot{m}_f + \left[\gamma\left(t\right) + \varphi\left(t\right)\right] \cdot \dot{x}\left(t\right). \tag{8}$$

In Equation (8), $\gamma(t)$ is the co-state and $\varphi(t)$ is the working mode coefficient of the battery. The specific expression is listed as follows:

$$\varphi\left(t\right) = \begin{cases} \varphi_B : & SoC \geq SoC_H \\ -\varphi_B : & SoC \leq SoC_L \\ 0 : & \text{else} \end{cases}, \tag{9}$$

where SoC_H is the upper limit of SoC, and SoC_L is the lower limit of SoC for the battery working mode; the working mode coefficient of the battery $\varphi(t)$ is set to limit SoC within the working mode.

The power distribution for the minimum fuel consumption rate based on PMP should meet the following conditions [16,17]:

1. At the duration $[t_0, t_f]$ of a driving cycle, an optimal control variable $u(t) \in [P_{B\_min}, P_{B\_max}]$ exists, which enables the Hamiltonian function $H(x^*, u^*, \gamma^*, \varphi^*, t)$ to be a global optimal solution.
2. Meanwhile, $x^*(t)$ and $\gamma^*(t)$ should satisfy the following canonical equations:

$$\dot{x}^*(t) = \frac{\partial H^*}{\partial \gamma}, \tag{10}$$

$$\dot{\gamma}^*(t) = -\frac{\partial H^*}{\partial x}. \tag{11}$$

Therefore, $H(x^*, u^*, \gamma^*, \varphi^*, t) = \min H[x, u, \gamma, \varphi, t]$ and $u(t) \in [P_{B\_min}, P_{B\_max}]$. The optimal control variable is $u^* = \arg\min H[x, u, \gamma, \varphi, t]$, and the desired u^* is the optimal power distributed by the battery. Hence, the alternator power should be the difference between the load power and the battery power.

4.3. Acquisition of the Co-State $\gamma(t)$

According to Equation (8), $\gamma(t)$ is the penalty factor of the SoC change rate, and the changes of $\gamma(t)$ affect the SoC changes. The constrained conditions of Equation (7) indicate that the acquisition of $\gamma(t)$ is a problem of two-point boundary values. Generally, the shooting method is used to solve the problem by converting it into an initial value problem [18]. In this method, the initial co-state of $\gamma(t)$, i.e., γ_0, can be determined by repeatedly trying until the final states satisfy the boundary condition, as shown in Figure 8. If the initial state SoC_0 is known, and γ_0 is set as a value, then the final state SoC_f is obtained by solving differential Equation (5). If SoC_0 is not equal to SoC_0, then γ_0 is updated and the process is repeated until $SoC_f = SoC_0$.

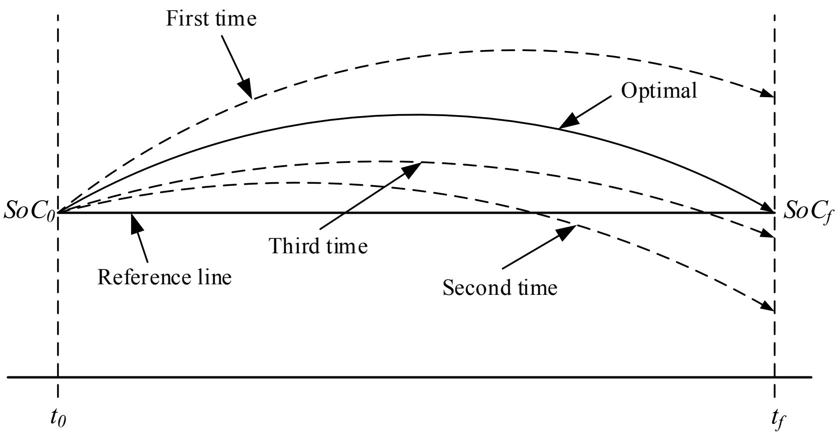

Figure 8. Trajectory of the shooting method.

For a specific driving cycle, if the load power change is known, γ_0 can be calculated offline by using the given shooting method. An algorithm to calculate γ_0 offline corresponding to a particular load power is presented in Figure 9. The algorithm inputs are SoC_0, load power P_L, fuel consumption rate set in the time $[t_0, t_f]$ of the given driving cycle, and calculation constants δ and ξ. The main process of the algorithm is detailed as follows:

1. The upper and lower limits of u are set according to P_L: $u_{\max} = \min[P_L, P_{B\_max}]$ and $u_{\min} = \max[P_L - P_{G\_max}, P_{B\_min}]$.

2. Set $\Delta u = [u_{\max} - u_{\min}]/n$ and discretize $u \in [u_{\min}, u_{\max}]$ as $u_i = u_{\min} + i{\cdot}\Delta u$, $i = 0, 1, 2, \ldots, n$.
3. For a given γ_0, calculate the Hamiltonian function H_i for each u_i at t_k by Equation (8).
4. Select $u^*(t_k) = \arg\min\{H_1, \ldots, H_i, \ldots, H_n\}$ and calculate the current $SoC(t_k)$.
5. Repeat steps (1)–(4) until the driving cycle is over, i.e., $t_k = t_f$.
6. Check whether $|SoC_f - SoC_0| > \xi$. If it is false, return the current γ_0; otherwise, update γ_0 and repeat steps (1)–(6) until a valid γ_0 is obtained.

Input: SoC_0, load power P_L, fuel consumption rate set $\{\dot{m}_f^{t_0}, \dot{m}_f^{t_1}, \ldots, \dot{m}_f^{t_f}\}$ from t_0 to t_f, constant δ, ξ

begin
  initialize $SoC_f = SoC_0 + \delta$ and $\delta > \xi$;
  set $u_{\max} = \min[P_L, P_{B\_\max}]$;
  set $u_{\min} = \max[P_L - P_{G\_max}, P_{B\_\min}]$;
  set $\Delta u = [u_{\max} - u_{\min}]/n$;
  while $|SoC_f - SoC_0| > \xi$ **do**
    update γ_0 to a new value;
    for $t_k \in \{t_0, t_1, \ldots, t_f\}$ **do**
      for $i \in \{0, 1, 2, 3, \ldots, n\}$ **do**
        $u_i = u_{\min} + i \cdot \Delta u$;
        calculate H_i by $u_i, \dot{m}_f^{t_k}$ and Equation (8);
      end for
      $u^*(t_k)$ =arg min{ $H_1, \ldots, H_i, \ldots, H_n$};
      calculate $SoC(t_k)$ by Equations (5), (6);
    end for
    $SoC_f = SoC_0$;
  end while
  return γ_0;
end

Figure 9. Algorithm of the initial co-state acquisition.

4.4. Strategy Implementation in Energy Management Controller

According to the real scenarios of electrical load use, the requirements of load powers in a vehicle can be divided into several grades, which are denoted as the load power set $\mathbf{P} = \{P_L^0, P_L^1, \ldots, P_L^m\}$. For $\forall P_L^i \in \mathbf{P}$, the algorithm in Figure 9 can be used to find its corresponding initial co-state γ_0^i if the driving cycle is given. Set $\gamma_0 = \{\gamma_0^1, \gamma_0^2, \ldots, \gamma_0^m\}$ is the initial co-state set, which corresponds to $\mathbf{P}$. $\mathbf{P}$ and γ_0 are used to implement the aforementioned strategy in an energy management controller. The working process of the strategy is shown in Figure 10.

In Figure 10, the BCM monitors the working state of electrical loads in the vehicle, and the SoC(t) of the battery is measured by the IBS in real-time. The EMS collects the rotational speed $n(t)$ and torque $T(t)$ of the engine, which are used to calculate the fuel consumption rate $\dot{m}_f(t)$. First, the energy management controller calculates the current requirements of load power P_L^i based on the information from BCM and finds the corresponding initial co-state γ_0^i in γ_0. Next, the Hamiltonian function H_i corresponding to each $u_i \in [u_{\min}, u_{\max}]$ is calculated through SoC(t), $\dot{m}_f(t)$, and γ_0^i. Then, the desired output power of the battery is chosen as u^*, which makes the Hamiltonian function H_i the minimum. Therefore, the desired output power of the alternator is obtained as $P_L^i - u*$. Finally, this output power of the alternator is converted into the control signal of the voltage based on the model in Figure 4, and the control signal is sent to the intelligent alternator to adjust its output power.

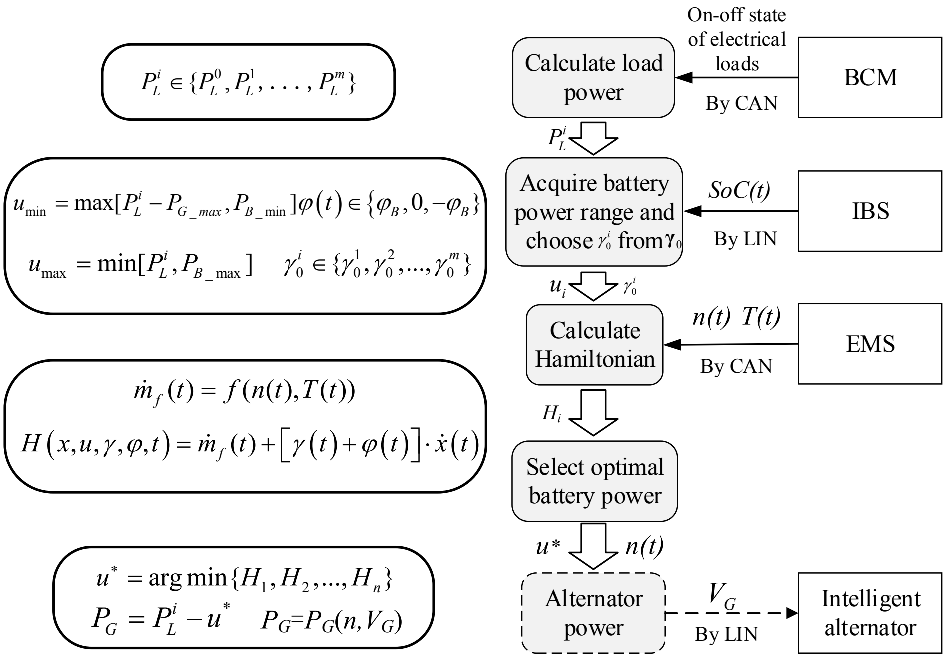

Figure 10. Working process of the strategy.

5. Experimental Results and Analysis

To validate the proposed method in this paper, different experiments are conducted on the vehicle platform, which is shown in Figure 11. The vehicle platform consists of chassis dynamometer, experimental passenger vehicle, and related instruments. The passenger vehicle is equipped with the proposed energy management controller, the IBS, which is designed by Hella (Lippstadt, Germany). The intelligent alternator is developed by Bosch (Stuttgart, Germany). Two current sensors and two voltage sensors are employed to measure the current and voltage of the battery and the intelligent alternator. These real-time data are collected by DAQ devices from National Instruments (Texas, TX, USA), and Vector CANoe (Vector, Stuttgart, Germany) is used to monitor the information in CAN and LIN buses.

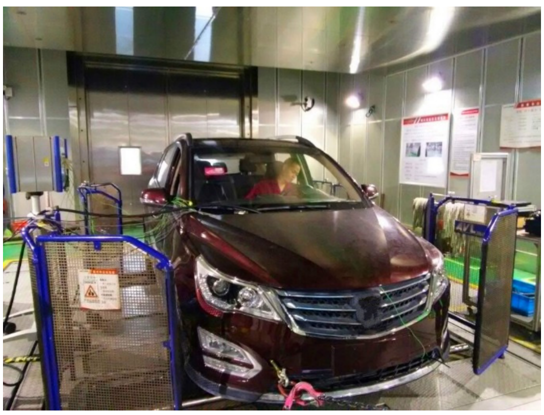

Figure 11. Vehicle platform.

Two driving cycles are applied for the experiments on the platform. The Economic Commission for Europe (ECE15) [9] and New European Driving Cycle (NEDC) [11] are shown in and Figure 12. Under ECE15, the experiment is carried out with constant electrical load power. The other experiment is carried out with changing load power under the NEDC.

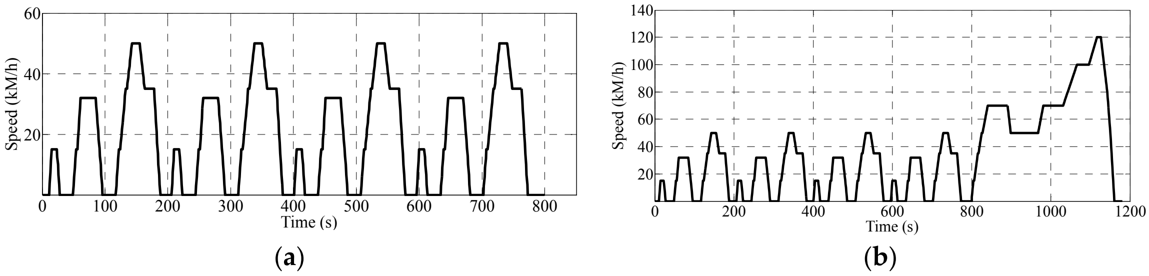

Figure 12. ECE15 and NEDC: (**a**) ECE15; and (**b**) NEDC.

5.1. Experiment with Constant Electrical Load Power

Under the ECE15, the experiment with constant electrical load power is conducted. When load power is 0.7 kW, the initial co-state with the shooting method is $\gamma^*(t) = -58$. When $\Delta SoC = 0$, the solution is optimal when $\gamma(t)$ satisfies all of the constrained conditions of PMP, including the constraint of Equation (7) on battery SoC.

Figure 13 presents the experiment results, which indicates that the energy management strategy of optimal power distribution (OPD) limits the SoC fluctuation of the battery. The final state differs slightly from the initial state and meets Equation (7). When the vehicle speeds up, the intelligent alternator decreases the output voltage, and the battery becomes the primary power supply and results in an effective increase of vehicle dynamic performance; when the vehicle slows down, the intelligent alternator increases output power, and the battery is charged rapidly to recycle and store kinetic energy into the battery.

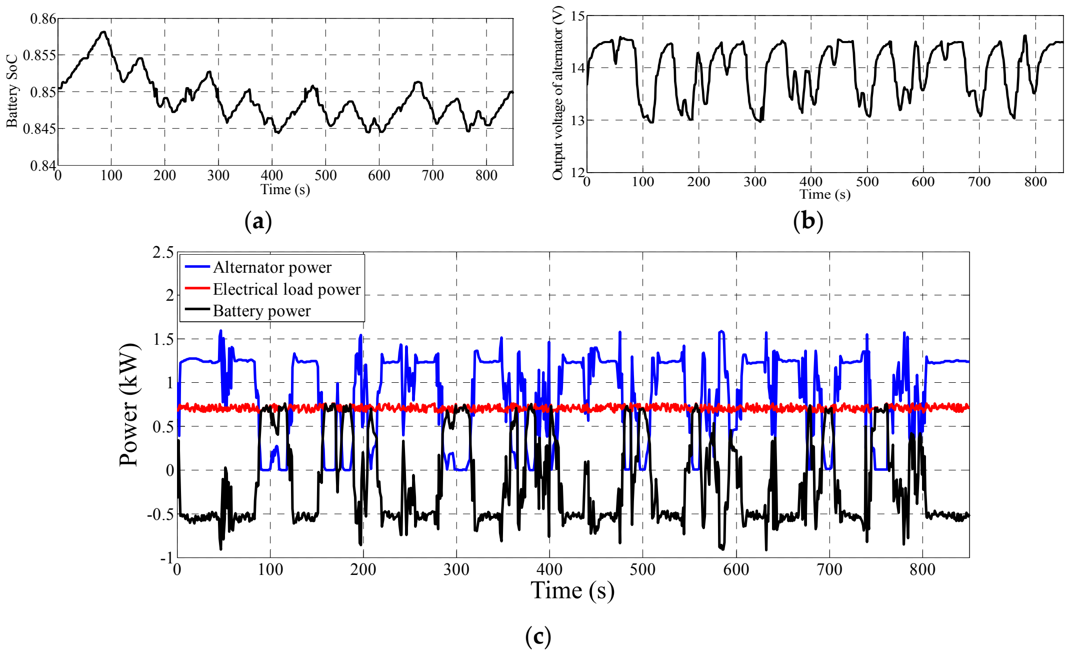

Figure 13. Results under the OPD strategy for the ECE15: (**a**) battery SoC; and (**b**) output voltage of the alternator; (**c**) the power change comparison.

To verify the OPD strategy, the same experiment is conducted in the vehicle without an energy management system, which is called the open-loop control (OLC) strategy. Figure 14 indicates that the battery is being charged often in the OLC strategy. The battery power being charged is approximately 0.3 kW, while the alternator power is around 1 kW, which is exactly the sum of the electrical load power and the battery charge power.

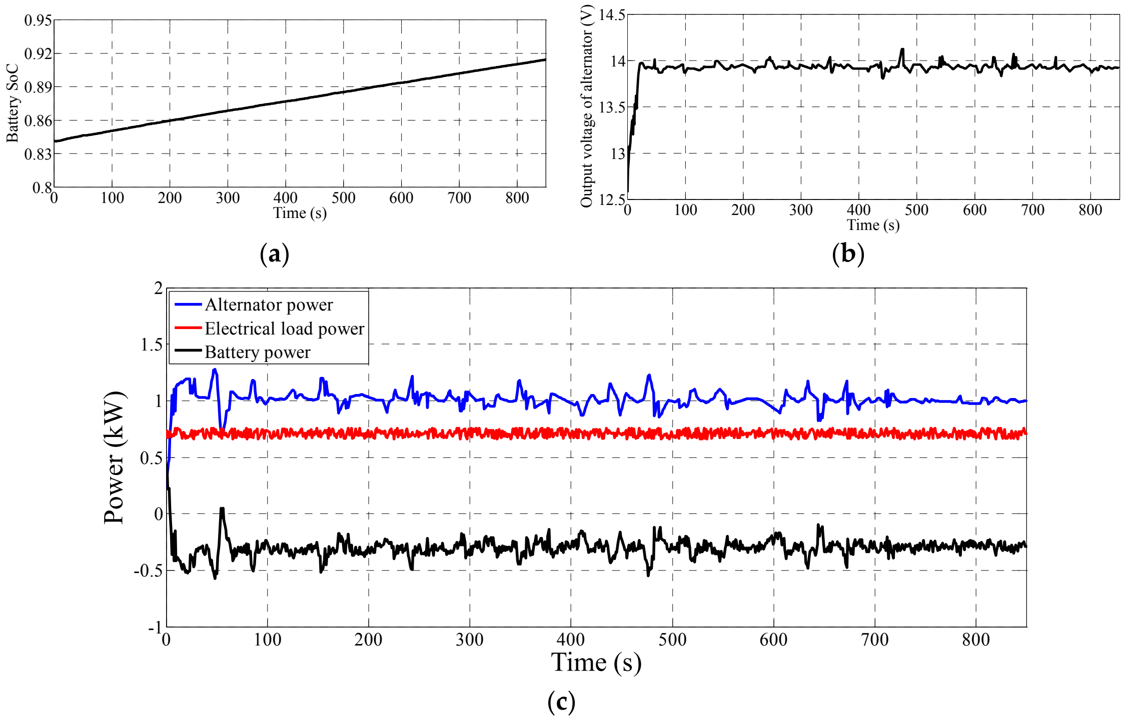

Figure 14. Results under the OLC strategy for the ECE15: (**a**) battery SoC; (**b**) output voltage of alternator; and (**c**) the power change comparison.

A comparison of the output voltages in Figures 13 and 14 show that the OPD strategy causes the alternator voltage to fluctuate fiercely, while the OLC strategy maintains the voltage stability at around 14 V. The alternator power is adjusted by a voltage change to reduce fuel consumption. This condition also improves the utilization efficiency caused by repeatedly charging and discharging the battery. The comparison of fuel consumption of OPD and OLC is presented in Table 1. For 100 km, OPD consumes 0.15 L fuel less than OLC, and the fuel saving rate is approximately 1.9%.

Table 1. Fuel consumption of constant electrical load power.

Control Strategy	Distance (km)	Fuel Consumption (mL)	Fuel Consumption (L/100 km)
OPD strategy	4.055	319.12	7.87
OLC strategy	4.049	324.73	8.02

5.2. Experiment with Changing Load Power

Under the NEDC, an experiment with changing load power is conducted. Figure 15 shows the power curves of the battery, alternator, electrical load, and output voltage curve of the alternator. The experiment results are similar to those of the experiment with unchanged load power. For the change of vehicle electrical appliances, the output voltage of the alternator is maintained between 13 V and 14.8 V; the battery SoC can fluctuate within a certain range; and the final SoC is almost equal to the initial SoC. However, the total output power from the battery and alternator is almost equal to the load power. This condition denotes that the energy management controller with the OPD strategy can distribute the demand of load power in real-time to the battery and the alternator, thereby decreasing the fuel consumption from the alternator.

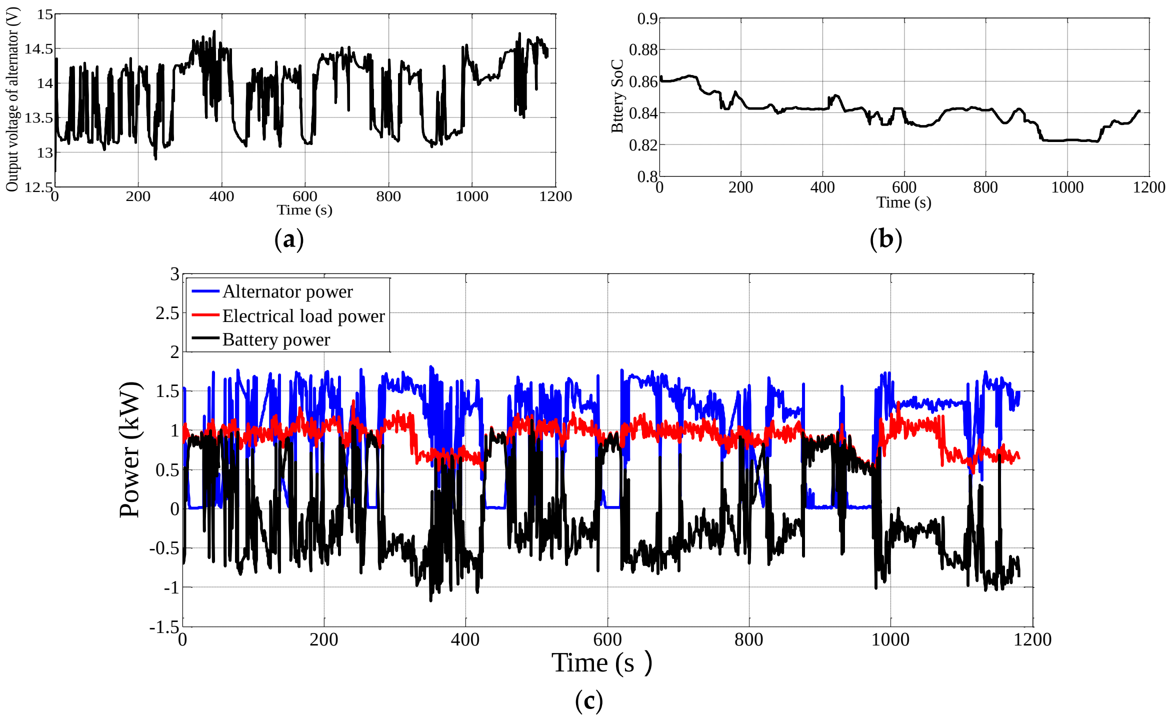

Figure 15. Results under the OLC strategy for the NEDC: (**a**) output voltage of alternator; (**b**) battery SoC; and (**c**) the power change comparison.

Table 2 presents a comparison of the fuel consumption of OPD and OLC under the NEDC. For 100 km, OPD consumes 0.14 L fuel less than OLC, and the fuel saving rate is about 1.7%. All of the results demonstrate that the OPD strategy can effectively reduce vehicle fuel consumption and increase vehicle fuel economy.

Table 2. Fuel consumption of changing load power.

Control Strategy	Distance (km)	Fuel Consumption (mL)	Fuel Consumption (L/100km)
OPD strategy	10.958	867.87	7.92
OLC strategy	10.961	883.46	8.06

Furthermore, Table 3 lists the improved effects of fuel economy from the A-PMP (Adaptive PMP) strategy in [9] and the OPD strategy in this paper. The A-PMP strategy in [9] can increase fuel economy by almost 1.4% while the OPD strategy in this paper can increase fuel economy by almost 1.7%. The improvement of fuel economy from the A-PMP and the OPD is very close. However, the implementation of A-PMP relies on modifying the structure of the alternator controller. It is much more complicated than the implementation of OPD based on an intelligent alternator. Therefore, OPD is superior to A-PMP on the implementation and engineering application.

Table 3. The comparison of fuel economy improvement.

Control Strategy	Fuel Consumption (L/100 km)	Fuel Economy Improvement
A-PMP strategy [9]	10.69	1.4%
EVR strategy [9]	10.84	
OPD strategy	7.92	1.7%
OLC strategy	8.06	

6. Conclusions

For the electrical system of ICE vehicles, an energy management system is investigated, and a real-time control strategy of the energy management in this system is proposed. The control strategy can appropriately distribute output power of the intelligent alternator and battery power according to the electrical load and driving cycle. The experimental results demonstrate that, compared with the widely-applied OLC strategy, the proposed OPD strategy leads to improved fuel economy. In the future, the electrical model of the vehicle power supply system will be studied in depth, with emphasis on methods to reduce the calculation complexity of the OPD strategy. This type of research will help accelerate the practical application of the energy management system in ICE vehicles.

Acknowledgments: This work was finically supported by the National Natural Science Foundation of China (No. 61202096) and the Scientific and Technological Special Project of Anhui Province (No.15czz02039). This paper was also generously supported by the Scientific Research Foundation for the Returned Overseas Chinese Scholars of State Education Ministry (No. [2013]693) the Natural Science Foundation of Higher Education Institutions of Anhui Province (No. KJ2012A226) and the Fundamental Research Funds for the Central Universities (No. 2013HGCH0014). This work was also sponsored by Project of JiangHuai Auto Company (No. W2014JSKF0086, No. W2016JSKF0096).

Author Contributions: Yuefei Wang designed the main parts of the study, including the models, implementation of algorithm and the working process of the strategy. Hao Hu and Xuhui Sun designed and performed the experiments under the supervision of Yuefei Wang. Li Zhang arranged and analyzed all the data. Yuefei Wang and Hao Hu also made the article structure and Nan Zhang contributed to part of the writing and editing work of manuscript.

Conflicts of Interest: The authors declare no conflict of interest.

References

1. Fabio, C.; Marcello, C. A review of energy consumption, management, and recovery in automotive systems, with considerations of future trend. *J. Automob. Eng.* **2013**, *227*, 914–936.
2. Zheng, C.; Chunting, C.M.; Xia, B.; You, C.W. Energy management of power-split plug-in hybrid electric vehicles based on simulated annealing and Pontryagin's minimum principle. *J. Power Sources* **2013**, *272*, 160–168.
3. Hanane, H.; Jamel, G.; Ahmed, C. Combination of Markov chain and optimal control solved by Pontryagin's Minimum Principle for a fuel cell/supercapacitor vehicle. *Energy Convers. Manag.* **2015**, *91*, 387–393.
4. Hou, C.; Ouyang, M.G.; Xu, L.F.; Wang, H.W. Approximate Pontryagin's minimum principle applied to the energy management of plug-in hybrid electric vehicles. *Appl. Energy* **2013**, *115*, 174–189. [CrossRef]
5. Simona, O.; Laura, T. Adaptive Pontryagin's Minimum Principle supervisory controller design for the plug-in hybrid GM Chevrolet Volt. *Appl. Energy* **2015**, *147*, 224–234.
6. Zou, Y.; Liu, T.; Sun, F.C.; Peng, H. Comparative study of dynamic programming and Pontryagin's Minimum Principle on energy management for a Parallel Hybrid Electric Vehicle. *Energies* **2013**, *6*, 2305–2318.
7. Kong, W.W.; Yang, D.G.; Li, B.; Lian, X.M. Intelligent control and reformation for conventional automotive generators. *J. Tsinghua Univ. (Sci. Technol.)* **2014**, *54*, 738–743.
8. Kong, W.W.; Yang, D.G.; Li, B.; Lian, X.M. A research on the management method of automotive battery. *Automot. Eng.* **2015**, *37*, 576–581.
9. Colin, W.; Sabarish, G.; Lisa, F.; Marcello, C. A model-based supervisory energy management strategy for a 12V vehicle electrical system. *Control Eng. Pract.* **2015**, *44*, 20–30.

10. Jeremy, C.; Lisa, F.; Marcello, C. An ECMS-Based approach for the energy management of a vehicle electrical system. *IFAC Proc. Vol.* **2013**, *46*, 115–120.
11. Wang, Y.F.; Wang, H.R.; Hu, H.; Huang, L. Research of energy management system in vehicle based on double fuzzy control. *J. Electron. Meas. Instrum.* **2015**, *29*, 1790–1797.
12. He, H.W.; Xiong, R.; Fan, J.X. Evaluation of lithium-ion battery equivalent circuit models for state of charge estimation by an experimental approach. *Energies* **2011**, *4*, 582–598. [CrossRef]
13. Daniel, L.; Brian, S. Lead-acid state of charge estimation for start-stop applications. *SAE Int. J. Altern. Powertrains* **2013**, *2*, 172–178.
14. Wang, Y.F.; Fang, H.T.; Wang, B.; Liu, H.J. Highly precise determination of the state of charge of vehicular battery. *Instrum. Sci. Technol.* **2016**, *44*, 445–457. [CrossRef]
15. Namwook, K.; Sukwon, C.; Peng, H. Optimal Control of Hybrid Electric Vehicles Based on Pontryagin's Minimum Principle. *Control Syst. Technol.* **2011**, *19*, 1279–1287. [CrossRef]
16. Jongryeol, J.; Daeheung, L.; Namwook, K.; Zheng, C.H.; Park, Y.I.; Cha, S.W. Development of PMP-based power management strategy for a parallel hybrid electric bus. *Int. J. Precis. Eng. Manuf.* **2013**, *15*, 345–353.
17. Hanane, H.; Jamel, G.; Ahmed, C. An optimal control solved by Pontryagin's Minimum Principle approach for a fuel cell/supercapacitor vehicle. In Proceedings of the Electrical Power and Energy Conference (EPEC), Calgary, AB, Canada, 12–14 November 2014; pp. 87–92.
18. Kim, N.W.; Lee, D.H.; Zheng, C.; Shin, C.; Seo, H.; Cha, S.W. Realization of PMP-based control for hybrid electric vehicles in a backward-looking simulation. *Int. J. Automot. Technol.* **2013**, *15*, 625–635. [CrossRef]